Artifact Assessment Approaches for Images

Gwanggil Jeon

Department of Embedded Systems Engineering, Incheon National University
12-1 Songdo-dong, Yeonsu-gu, Incheon 406-772, Korea
gjeon@incheon.ac.kr

Abstract

In this paper, we proposed a new artifact level estimation algorithm. The noise model is firstly proposed and 2D discrete wavelet transform is explained. The proposed method is based on Donoho's approach. From the result section, it is obvious that the proposed method gives favorable results.

Keywords: *mean, variance, noise, CFA, artifact*

1. Introduction

An image can be contaminated by noise in many ways with various steps such as image acquisition, recording, and transmission [1]. Thus, the artifacts estimation caused by noise can its removal process are important issue in image processing field [2, 3]. Every digital camera produces faultiness in images known as noise, which come into view as undesirable dots, lines and smears of color. An immoderate amount of noise spoils an image by taking attention away from the picture quality. From the other point of view, too much noise removal ruins pictures sharpness and detail, this should be compromised.

There have been several techniques that planned noise removal issue [6-11]. These approaches are classified into two classes: block-based methods and filter-based methods [12-33]. The preceding ones take into account few candidates which are considered to be intensity-homogeneous blocks. Here, noise variances are computed from intensity-homogeneous blocks, and the principal concern is how to conclude the intensity-homogeneous blocks. On the other hand, filter-based methods are conducted in different way. The noisy signal is removed by low-pass filters. After that the noise variance is computed from the difference between the noisy image and the low-pass filtered image. However, filter-based methods are not able to yield favorable results when the signal has complicated textures or structures due to the determined noise may be the image details.

This paper proposes artifact estimation algorithm to achieve correct noise reduction. The remaining of this paper is organized as follows. In Section 2, we explain noise model. Section 3 explains 2D discrete wavelet transform. Section 4 shows the experimental results, and Section 5 concludes the paper.

2. Noise Model

Generally, an image can be contaminated by zero-mean, additive white Gaussian noise with anonymous deviation σ_n. Then the noisy image can be modeled as,

$$I(n) = S(n) + \eta(n) \tag{1}$$

where $I(n)$ is the monitored noisy image, $S(n)$ is the original image, and $\eta(n)$ is the noisy signal at time instant n. To estimate artifact level of noisy CFA image, one can add noise during the process before white balance as shown in Figure 1.

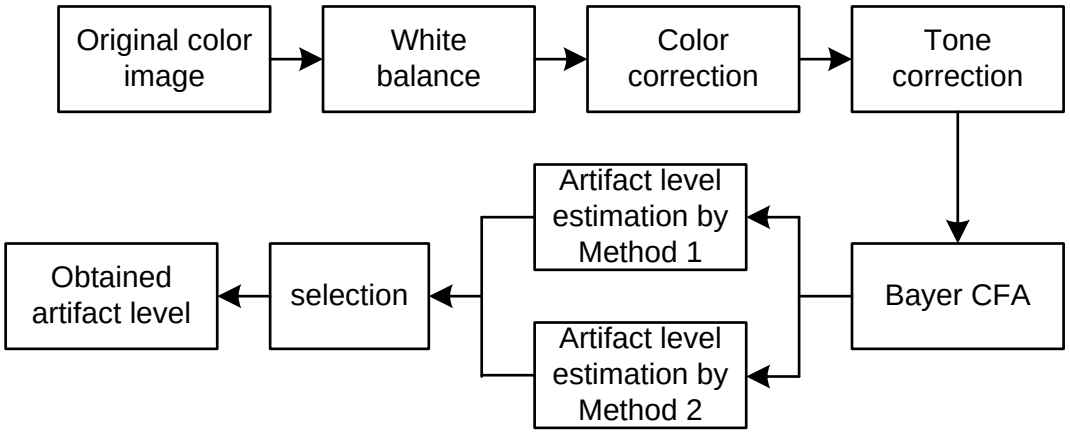

Figure 1. Flowchart of estimation of noisy Bayer CFA. The original color is input, and artifact level is calculated by the proposed methods

The noisy Bayer CFA is obtained as,

```
ORIG = im2double(imread(imagename));
S = size(ORIG); N1 = S(1); N2 = S(2);
randn('state',0); noi=randn(N1,N2,3); noi=noi/255;
teta = sigma*noi; RGBn = ORIG + teta;
CFAN(1:2:N1,2:2:N2) = RGBn(1:2:N1,2:2:N2,1);
CFAN(1:2:N1,1:2:N2) = RGBn(1:2:N1,1:2:N2,2);
CFAN(2:2:N1,2:2:N2) = RGBn(2:2:N1,2:2:N2,2);
CFAN(2:2:N1,1:2:N2) = RGBn(2:2:N1,1:2:N2,3);
```

3. 2D Discrete Wavelet Transform (DWT)

A 2D DWT is any wavelet transform where the wavelets are discontinuously chosen. As with other wavelet transforms, a significant promote it has over conventional transform such as Fourier transforms is temporal resolution. DWT takes both location and frequency information. There are two DWT are widely used, and they are Haar wavelets and Daubechies wavelets. The Haar wavelets was introduced by Alfréd Haar who was Jewish Hungarian mathematician. The inputs are lists of 2^n numbers, and the Haar wavelet transform was popular for its simplicity because it was designed to make a couple of input values, collecting the dissimilarity and summering the result. The Haar wavelet transform is conducted recursively. Finally the results are summarized with 2^{n-1} differences and one final sum. The Daubechies wavelet transform is one of the widely used transforms. This transform was invented by Belgian mathematician Ingrid Daubechies in 1988. This transform is based on the utilize of repetition relationship to create gradually delicate discrete samplings of an

implicit basis wavelet function. Note that each resolution is halved compared to that of the previous scale.

The 2D Fourier transform, the basis are represented as Eq. (1),

$$e^{j(w_1 t_1 + w_2 t_2)} \tag{1}$$

As can be seen in Eq. (1), the transformed coefficients are two variable functions in a matter that the 2D wavelet transforms. The wavelet and scaling function (SF) are both variable functions (VF), which are represented as $\psi(x,y)$ and $\varphi(x,y)$, respectively. The basis functions can be represented as

$$\begin{aligned} \varphi_{j,m,n}(x,y) &= 2^{j/2}\varphi\left(2^j x - m, 2^j y - n\right), \\ \psi^i_{j,m,n}(x,y) &= 2^{j/2}\psi^i\left(2^j x - m, 2^j y - n\right), \end{aligned} \tag{2}$$

where i={Ho,Ve,Di}, Ho, Ve, and Di stand for horizontal, vertical and diagonal, respectively. There are three wavelet functions, $\psi^H(x,y)$, $\psi^V(x,y)$, and $\psi^D(x,y)$. The SF is the low frequency form of the previous SF in two dimensions, thus there are one 2D SF. However, the wavelet function is identifying with the order to implement the filters. When the wavelet function meets Eq. (3), the function is separable.

$$f(x,y) = f_{Ho}(x)\, f_{Ve}(y). \tag{3}$$

These functions can be easily rewritten as Eq. (4),

$$\begin{aligned} \varphi(x,y) &= \varphi(x)\varphi(y), \\ \psi^{Ho}(x,y) &= \psi(x)\varphi(y), \\ \psi^{Ve}(x,y) &= \varphi(x)\psi(y), \\ \psi^{Di}(x,y) &= \psi(x)\psi(y). \end{aligned} \tag{4}$$

The outline of 2D wavelet transform can be drawn as Figure 2.

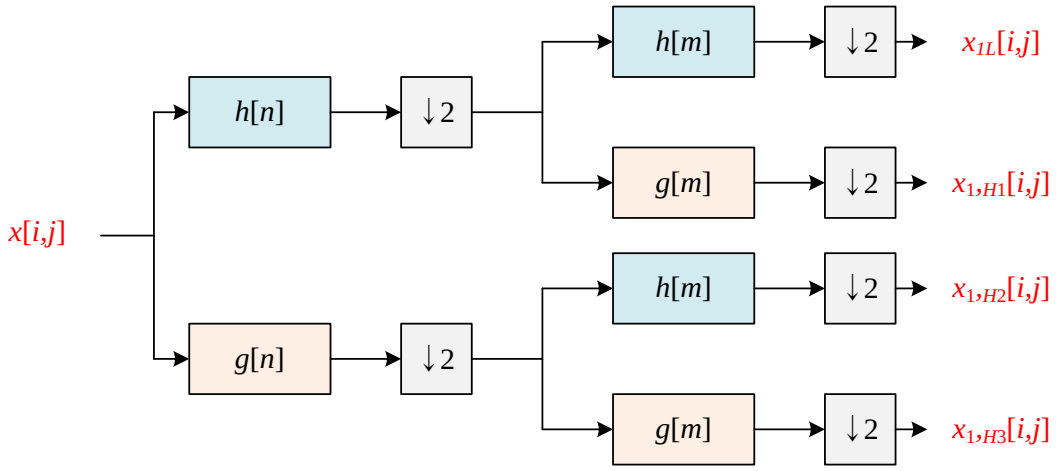

Figure 2. The outline of 2D wavelet transform

As we can see, Figure 2 shows the general form of 2D wavelet transform. Once the scaling function and the wavelet function are separable, the results can be separated into two steps. The first step can be conducted along the *i*-axis and then compute in the direction of the *j*-axis. For each axis, we can implement fast wavelet transform for fast simulation. Figure 3 shows an example of the 2D discrete wavelet transform. Figure 3(a) is the original image, and a diagrammatic diagram is shown in Figure 3(b), where the two dimensional signal is separated into subbands, and they are left-top (LL), right-top (HL), left-bottom (LH), and right-bottom (HH).

In [11], the noise level was estimated in two ways,

$$\sigma_1 = \frac{Median(w)}{\kappa} \tag{5}$$

or

$$\sigma_2 = \sqrt{\frac{\sum_{i=1}^{N}\sum_{j=1}^{M}\{w(i,j)\}^2}{N \cdot M}}. \tag{6}$$

Here, κ=0.6475. Parameter w is the diagonal sub-band at the first stage, *i.e.*, Di. We assume these results as Donoho1 (σ_1) and Donoho2 (σ_2), respectively. To make reliable results, we substracted the difference between ground truth and estimated σ_1 and σ_2. We assume these results are method1 and method2, respectively.

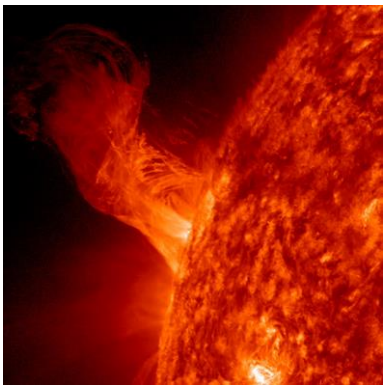

(a)

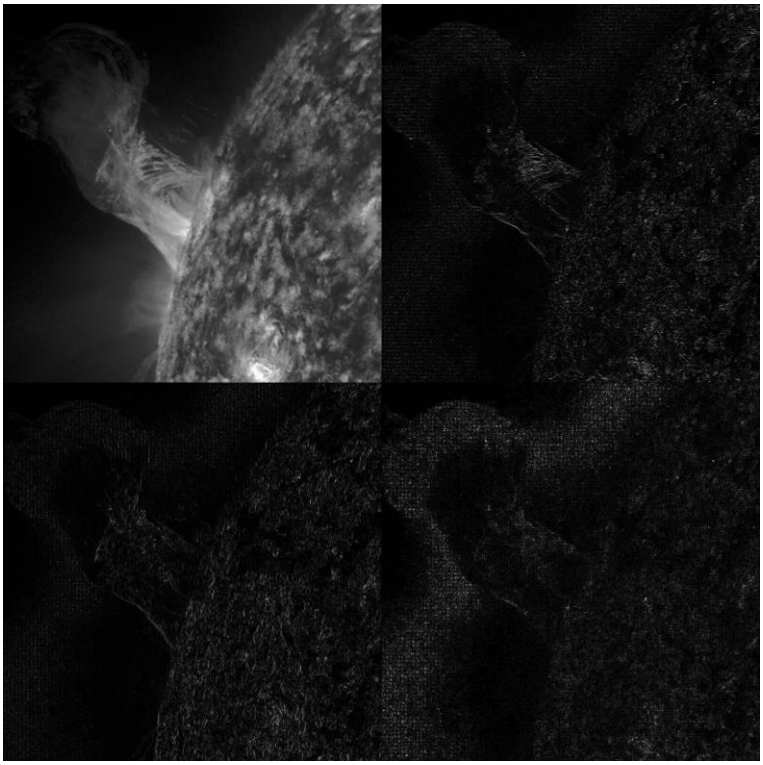

(b)

Figure 3. (a) Original image, (b) 2D discrete wavelet transform

4. Experimental Results

The proposed methods were tested on the LC dataset [34] that was used in a recent articles. The test set consists of 10 images with either 720-by-540 or vice versa. Noises with different level are first added in Bayer CFA, and then artifact estimation approach is applied. The estimated results are compared to the original results (ground truth) and results are reported in simulation results figures. Figure 4 shows 10 test images. The left images are original images, and the right images are noisy Bayer CFA images.

Figure 4. Test images. Left: original LC images from 1 to 10. Right: noisy Bayer CFA images from 1 to 10

Table 1 and Table 2 show the simulation results of σ_1 and σ_2 on 10 LC images. Table 3 and Table 4 show the modified results with our proposed approach. Figure 5 shows the simulation results on 10 LC images.

Table 1. Simulation results of σ_1 on 10 LC images. Horizontal axis: image number. Vertical axis: added noise level

	1	2	3	4	5	6	7	8	9	10
0	6.178	7.722	9.266	10.129	14.621	9.832	29.285	7.722	26.181	13.127
2	6.779	8.265	9.786	10.654	14.520	9.976	29.136	7.757	26.181	13.839
4	8.292	9.726	11.132	11.493	15.123	10.979	29.249	8.429	26.255	15.376
6	10.032	11.572	12.714	12.848	16.169	12.304	29.656	9.698	26.288	17.117
8	11.820	13.136	14.512	14.237	17.195	13.732	30.279	11.285	26.459	19.026
10	13.601	14.440	16.016	15.638	18.357	15.172	30.811	13.059	26.753	20.893
12	15.580	15.488	17.858	17.261	19.582	16.655	31.427	14.941	27.426	22.766
14	17.471	17.078	19.259	18.598	20.903	18.098	31.791	16.872	28.296	24.577
16	19.462	18.941	20.789	19.961	22.120	19.542	32.458	18.829	28.967	26.291
18	21.454	20.984	22.270	21.466	23.351	20.995	32.978	20.781	30.823	27.896
20	23.490	23.046	23.593	22.846	24.540	22.377	33.583	22.549	32.670	29.306

Table 2. Simulation results of σ_2 on 10 LC images

	1	2	3	4	5	6	7	8	9	10
0	11.983	20.475	17.343	14.174	18.976	12.957	29.586	16.909	32.431	24.238
2	12.143	20.551	17.428	14.278	19.050	13.073	29.644	17.001	32.480	24.300
4	12.623	20.771	17.683	14.589	19.280	13.415	29.803	17.268	32.622	24.485
6	13.389	21.132	18.102	15.094	19.661	13.966	30.062	17.700	32.854	24.790
8	14.395	21.625	18.674	15.775	20.184	14.702	30.418	18.287	33.176	25.211
10	15.594	22.243	19.385	16.610	20.839	15.597	30.867	19.014	33.584	25.742
12	16.947	22.975	20.220	17.577	21.615	16.626	31.406	19.866	34.074	26.377
14	18.418	23.811	21.165	18.656	22.497	17.765	32.030	20.828	34.645	27.109
16	19.983	24.740	22.205	19.828	23.475	18.994	32.734	21.884	35.292	27.929
18	21.620	25.752	23.328	21.078	24.537	20.298	33.514	23.023	36.010	28.831
20	23.314	26.838	24.523	22.393	25.672	21.662	34.363	24.231	36.796	29.806

Table 3. Simulation results of modified σ_1 on 10 LC images

	1	2	3	4	5	6	7	8	9	10
0	2.164	3.140	3.157	4.208	5.850	4.408	8.317	3.911	8.336	2.198
2	6.779	8.265	9.786	10.654	14.520	9.976	29.136	7.757	26.181	13.839
4	8.292	9.726	11.132	11.493	15.123	10.979	29.249	8.429	26.255	15.376
6	9.032	9.572	9.714	8.848	11.169	6.304	22.656	1.698	17.288	7.117
8	9.656	9.996	11.355	10.029	11.345	9.324	21.962	7.374	18.123	16.828
10	6.822	6.175	6.230	4.984	3.837	5.196	1.675	5.302	0.572	7.054
12	7.288	5.762	6.726	5.768	4.459	5.676	2.178	6.512	1.171	7.390
14	8.439	7.506	9.545	9.750	9.734	11.794	9.135	15.174	11.008	17.460
16	9.806	8.945	9.434	9.932	10.775	10.218	10.496	11.455	10.844	9.463
18	14.632	14.809	16.040	16.482	19.514	15.799	31.303	15.479	30.251	20.842
20	16.202	17.284	16.867	17.078	20.081	16.701	31.405	16.037	31.499	21.916

Table 4. Simulation results of modified σ_2 on 10 LC images

	1	2	3	4	5	6	7	8	9	10
0	5.582	7.665	7.338	6.897	7.541	6.679	8.274	7.272	8.434	7.982
2	12.143	20.551	17.428	14.278	19.050	13.073	29.644	17.001	32.480	24.300
4	12.623	20.771	17.683	14.589	19.280	13.415	29.803	17.268	32.622	24.485
6	12.389	19.132	15.102	11.094	14.661	7.966	23.062	9.700	23.854	14.790
8	8.813	13.960	11.336	8.878	12.643	8.023	22.144	11.015	24.742	17.229
10	3.451	1.692	1.957	2.332	1.789	2.524	1.223	2.013	1.104	1.442
12	4.324	2.204	2.537	2.988	2.335	3.211	1.603	2.598	1.452	1.892
14	6.029	4.679	6.063	7.562	7.836	9.799	8.968	11.128	10.791	12.319
16	11.170	10.780	10.869	10.950	10.832	10.971	10.590	10.869	10.550	10.700
18	18.169	24.060	21.371	18.746	22.748	17.774	32.291	21.010	34.906	27.389
20	18.990	24.634	21.986	19.405	23.337	18.451	32.760	21.633	35.344	27.914

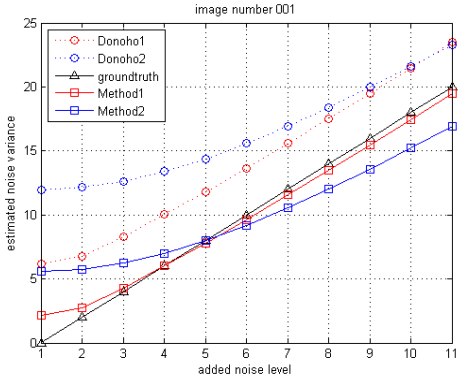

(a)

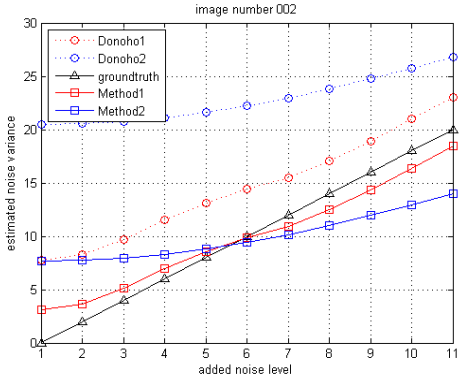

(b)

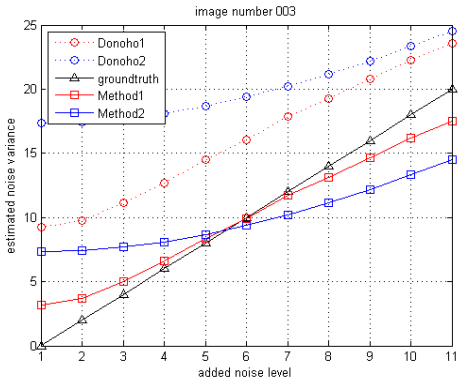

(c)

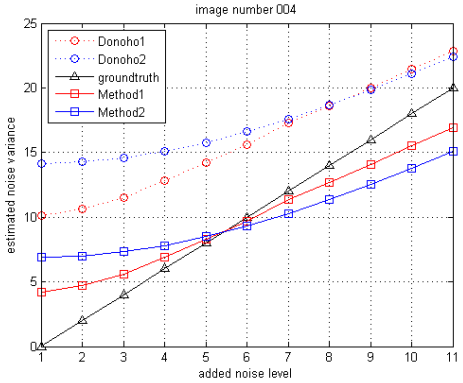

(d)

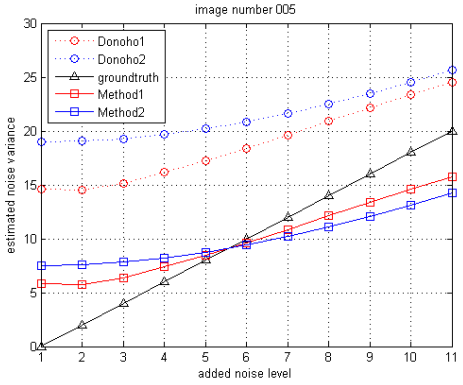
image number 005
Donoho1
Donoho2
groundtruth
Method1
Method2
estimated noise variance
added noise level

(e)

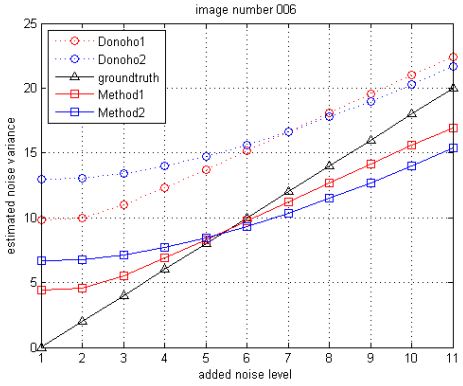
image number 006
Donoho1
Donoho2
groundtruth
Method1
Method2
estimated noise variance
added noise level

(f)

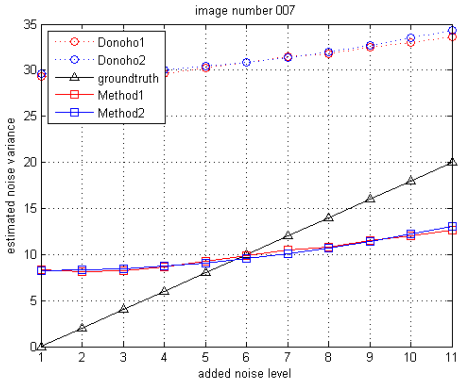
image number 007
Donoho1
Donoho2
groundtruth
Method1
Method2
estimated noise variance
added noise level

(g)

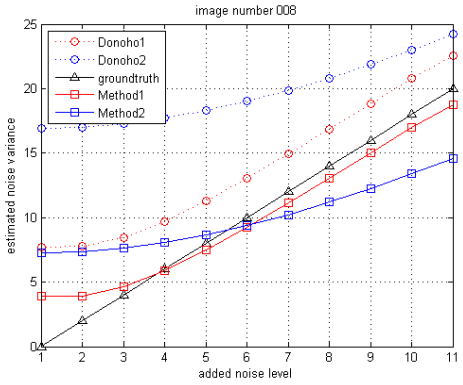
image number 008
Donoho1
Donoho2
groundtruth
Method1
Method2
estimated noise variance
added noise level

(h)

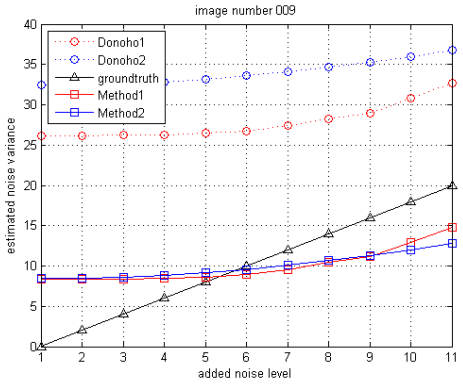
image number 009
Donoho1
Donoho2
groundtruth
Method1
Method2
estimated noise variance
added noise level

(i)

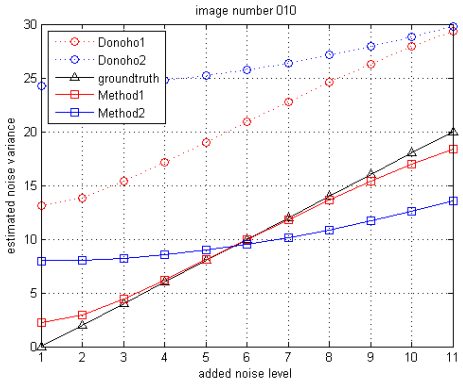
image number 010
Donoho1
Donoho2
groundtruth
Method1
Method2
estimated noise variance
added noise level

(j)

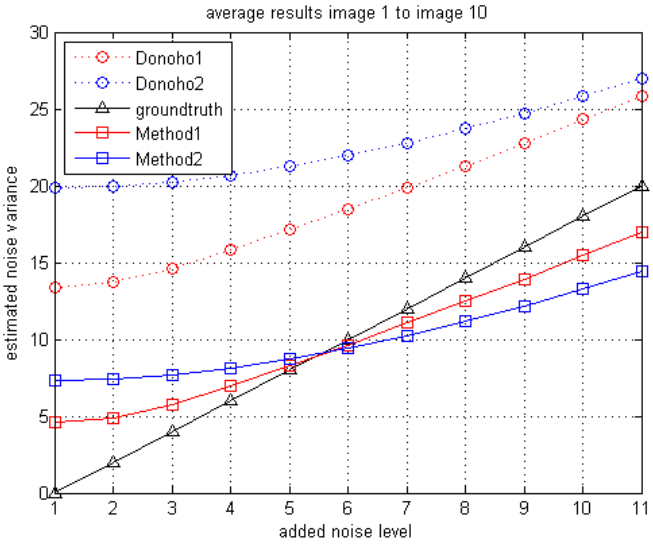

(k)

Figure 5. Simulation results on 10 LC images; (a-j) image number 1 to 10, (k) average results of 10 images

4. Conclusions

We propose a new artifact level estimation algorithm. The proposed method is based on Donoho's approach and wavelet transform. The diagonal sub-band was used for estimation noise level. By adding the difference between ground truth and estimated values, the results become better.

Acknowledgements

This work was supported in part by the National Science Foundation of China (NSFC) under Grant 61001100, 61077009.

References

[1] K. Rank, M. Lendl and R. Unbehauen, "Estimation of image noise variance", IEE Proceedings - Vision, Image, and Signal Processing, vol. 146, **(1999)**, pp. 80.
[2] A. Amer, A. Mitiche and E. Dubois, "Reliable and fast structure-oriented video noise estimation", International Conference on Image Processing, vol. 51, **(2002)**, pp. I–840–I–843.
[3] Z. Daniel and W. Yair, "Scale invariance and noise in natural images", 2009 IEEE 12th International Conference on Computer Vision, **(2009)**, pp. 2209–221.
[4] Z. Xiang and M. Peyman, "Automatic parameter selection for denoising algorithms using a no-reference measure of image content", IEEE trans. on image processing, vol. 19, **(2010)**, pp. 3116-32.
[5] K. Dabov, A. Foi, V. Katkovnik and K. Egiazarian, "Image denoising by sparse 3-d transformdomain collaborative filtering", IEEE transactions on image processing, **(2007)**, pp. 2080–95.
[6] L. Sendur and I. W. Selesnick, "Bivariate shrinkage functions for wavelet-based denoising exploiting interscale dependency", IEEE Trans. Signal Processing, vol. 50, **(2002)** November, pp. 2744-2756.
[7] B. Tang, G. Sapiro and V. Caselles, "Color image enhancement via chromaticity diffusion", IEEE Trans. Image Processing, vol. 10, **(2001)** May, pp. 701-707.
[8] K. J. Boo and N. K. Bose, "A motion-compensated spatio-temporal filter for image sequences with signal-dependent noise," IEEE Trans. Circuits Sys. Video Technol., vol. 8, **(1998)** June, pp. 287-298.

[9] S. Tai and S. Yang, "A fast method for image noise estimation using laplacian operator and adaptive edge detection", 2008 3rd International Symposium on Communications, Control and Signal Processing, **(2008)** March, pp. 1077–1081.
[10] D. Shin, R. Park, S. Yang and J. Jung, "Block-based noise estimation using adaptive gaussian filtering", IEEE Transactions on Consumer Electronics, vol. 51, **(2005)** February, pp. 218–226.
[11] D. L. Donoho and I. M. Johnstone, "Ideal spatial adaptation via wavelet shrinkage", Biometrika, vol. 81, **(1994)**, pp. 425-455.
[12] M. Anisetti, C. A. Ardagna, V. Bellandi, E. Damiani and S. Reale, "Advanced Localization of Mobile Terminal in Cellular Network", IJCNS, vol. 1, no. 1, **(2008)**, pp. 95-103.
[13] C.-T. Hsieh, Y.-K. Wu and K.-M. Hung, "Hybrid Watermarking Scheme for Halftone Images", International Journal of Advanced Science and Technology, **(2008)**, pp. 9-20.
[14] R. Adipranata, E. Cherry, G. Ballangan and R. P. Ongkodjojo, "Fast Method for Multiple Human Face Segmentation in Color Image", International Journal of Advanced Science and Technology, **(2009)**, pp. 19-32.
[15] D. Bhattacharyya, A. Roy, P. Roy and T.-h. Kim, "Receiver Compatible Data Hiding in Color Image", International Journal of Advanced Science and Technology, **(2009)**, pp. 15-24.
[16] M. Drahanský, "Realization of Experiments with Image Quality of Fingerprints", International Journal of Advanced Science and Technology, **(2009)**, pp. 79-88.
[17] B.V. Ramana Reddy, A. Suresh, M. Radhika Mani and V. Vijaya Kumar, "Classification of Textures Based on Features Extracted from Preprocessing Images on Random Windows", International Journal of Advanced Science and Technology, **(2009)**, pp. 9-18.
[18] W. Wu, Z. Liu and X. He, "Learning-based super resolution using kernel partial least squares", Image Vision Comput., vol. 29, **(2011)**, pp. 394-406.
[19] W. Wu, Z. Liu, W. Gueaieb and X. He, "Single-image super-resolution based on markov random field and contourlet transform", J. Electron. Imaging, vol. 20, 023005, **(2011)**.
[20] W. Wu, Z. Liu and D. Krys, "Improving laser image resolution for pitting corrosion measurement using markov random field method", Autom. Constr., vol. 21, **(2012)**, pp. 172-183.
[21] W. Wu, Z. Liu, M. Chen, X. Yang and X. He, "An automated vision system for container-code recognition", Expert Systems with Applications, vol. 39, **(2012)**, pp. 2842-285.
[22] W. Wu, X. Yang and X. He, "Handwritten numeral recognition by model reconstruction based on manifold learning", The 2007 International Conference on Information Computing and Automation (ICICA'07), **(2007)**.
[23] J. Wu, C. Liang, J. Han, Z. Hu, D. Huang, H. Hu, Y. Fang and L. Jiao, "A Two-Stage Lossless Compression Algorithm for Aurora Image Using Weighted Motion Compensation and Context-Based Model", Optics Communications, vol. 290, **(2012)** October 22, pp.19-27.
[24] Y. Fang, J. Wu and B. Huang, "2D sparse signal recovery via 2D orthogonal matching pursuit", Science China: Inf. Sci., vol. 55, **(2012)**, pp. 889-897.
[25] J. Wu, T. Li, T.-J. Hsieh, Y.-L. Chang and B. Huang, "Digital Signal Processor-based 3D Wavelet Error-resilient Lossless Compression of High-resolution Spectrometer Data", Journal of Applied Remote Sensing, Vol. 5, 051504, **(2011)** November 28.
[26] A. Paul, J. Wu, J.-F. Yang and J. Jeong, "Gradient-based edge detection for motion estimation in H.264/AVC", IET Image Processing, vol. 5, no. 4, **(2011)**, pp.323-327.
[27] J. Wu, J. Huang, G. Jeon, J. Jeong and L.C. Jiao, "An adaptive autoregressive de-interlacing method", Optical Engineering, vol. 5, no. 50, **(2011)**, pp. 057001.
[28] J. Wu, A. Paul, Y. Xing, Y. Fang, J. Jeong, L. Jiao and G. Shi, "Morphological dilation image coding with context weights prediction", Signal Processing: Image Communication, vol. 25, no. 10, **(2010)**, pp. 717-728.
[29] M. Anisetti, C. A. Ardagna, E. Damiani, F. Frati, H. A. Müller and A. Pahlevan, "Web Service Assurance", The Notion and the Issues. Future Internet, vol. 4, no. 1, **(2012)**, pp. 92-109.
[30] M. Anisetti, C. A. Ardagna, V. Bellandi, E. Damiani, M. Döller, F. Stegmaier, T. Rabl, H. Kosch and L. Brunie, "Landmark-assisted location and tracking in outdoor mobile network", Multimedia Tools Appl., vol. 59, no. 1, **(2012)**, pp. 89-11.
[31] M. Anisetti, C. A. Ardagna, E. Damiani and J. Maggesi, "Security certification-aware service discovery and selection", SOCA, **(2012)**, pp. 1-8.
[32] M. Anisetti, C. A. Ardagna and E. Damiani, "A Low-Cost Security Certification Scheme for Evolving Services", ICWS, **(2012)**, pp. 122-129.
[33] M. Anisetti, C. A. Ardagna, V. Bellandi, E. Damiani and S. Reale, "Map-Based Location and Tracking in Multipath Outdoor Mobile Networks", IEEE Transactions on Wireless Communications, vol. 10, no. 3, **(2011)**, pp. 814-824.
[34] The LC image dataset, http://www.gipsa-lab.grenoble-inp.fr/~laurent.condat/imagebase.html.

Author

Gwanggil Jeon received the BS, MS, and PhD (summa cum laude) degrees in Department of Electronics and Computer Engineering from Hanyang University, Seoul, Korea, in 2003, 2005, and 2008, respectively.

From 2008 to 2009, he was with the Department of Electronics and Computer Engineering, Hanyang University, from 2009 to 2011, he was with the School of Information Technology and Engineering (SITE), University of Ottawa, as a postdoctoral fellow, and from 2011 to 2012, he was with the Graduate School of Science & Technology, Niigata University, as an assistant professor. He is currently an assistant professor with the Department of Embedded Systems Engineering, Incheon National University, Incheon, Korea. His research interests fall under the umbrella of image processing, particularly image compression, motion estimation, demosaicking, and image enhancement as well as computational intelligence such as fuzzy and rough sets theories. He was the recipient of the IEEE Chester Sall Award in 2007 and the 2008 ETRI Journal Paper Award.